Harmonic Interaction Model for Fast and Accurate Cogging Torque Calculation in Permanent Magnet Machines

Litao Dai[1], Shuangxia Niu[1], Jian Gao[2], and Shoudao Huang[2]

[1] Department of Electrical and Electronic Engineering, The Hong Kong Polytechnic University, Hong Kong, 999077, China
[2] College of Electrical and Information Engineering, Hunan University, Changsha, 410002, China

This paper presents a semi-analytical model for predicting cogging torque based on harmonic interaction principle within the airgap. It derives the airgap's magnetic energy through Fourier expressions of the rotor magnetomotive force in motion and the airgap permeance considering slotting effects. The analytical expression for cogging torque is then obtained by differentiating the airgap magnetic energy with respect to motion. This model is distinguished by its fast computational speed and high accuracy compared to the finite element method, making it advantageous for large-scale design optimization. Notably, the model can analyze the factors influencing cogging torque, offering theoretical insights for cogging torque reduction.

***Index Terms*—Permanent magnet machines, cogging torque, analytical model, harmonic.**

I. Introduction

Cogging torque, an intrinsic yet undesirable trait of permanent magnet machines (PMMs), leads to torque ripples that can impact control accuracy and smooth operation. Predicting cogging torque is crucial for characterizing this phenomenon and implementing targeted reduction approaches [1]. Typically, cogging torque modeling involves a numerical approach based on the finite element method (FEM) [2] and an analytical method based on the energy approach [3].

The numerical method offers high accuracy in cogging torque calculations but is time-consuming, making it more suitable for motor verification rather than large-scale design optimization. On the other hand, analytical models are exceptionally fast and ideal for large-scale optimization tasks. However, ensuring accuracy, a crucial aspect of modeling, can be challenging. As a result, achieving accurate cogging torque modeling has been the subject of extensive research, yielding promising results [3].

The precision of the airgap flux density is a critical factor influencing the accuracy of analytical models. The sub-domain analytical model, which resolves the magnetic field boundary conditions in distinct regions, stands out for its ability to precisely forecast airgap flux density, enabling accurate cogging torque predictions [4], [5]. Over the past decades, extensive research has focused on sub-domain models to accommodate various surface-mounted PM (SPM) machine structures, encompassing factors like eccentric rotor shapes [6], magnet imperfections [7], manufacturing variations [8], among others. Moreover, investigations have delved into interior PM (IPM) machines with diverse rotor PM topologies, such as V-type [9], U-type [10], [11], and Delta-type PMs [12]. Apart from subdomain-based models, studies have explored the prediction of airgap flux densities in IPM machines through magnetic equivalent circuit models [13], [14], [15], [16].

While the aforementioned methods demonstrate excellent predictive capabilities for flux density and cogging torque calculations, they are not without limitations, as outlined below:

1. The modeling process is complex, making it challenging to promote widespread use of the methods.
2. The models lack strong universality; although various topologies have been studied, each comes with specific constraints that restrict their general applicability.
3. Structure features like chamfering of PMs and iron cores is difficult to consider. Errors in these features could significantly impact prediction accuracy, especially for fractional-slot motors where cogging torque is primarily generated by high-order field harmonics.
4. The existing models struggle to effectively capture the relationship between magnetic field harmonics and cogging torque, which hinders the exploration of new cogging torque suppression design methods.

Based on these challenges, this paper introduces for the first time a general and user-friendly cogging torque prediction model based on the principle of field harmonic interaction, clarifying the intrinsic relationship between cogging torque and field harmonics. This methodology holds applicability across SPM and IPM structures, leveraging the continued use of FEM. Notably, its distinguishing feature is the requirement for only two static field FEM calculations, complemented by the harmonic interaction model (HIM), which markedly accelerates computations. Consequently, this method proves effective in understanding cogging torque phenomena and developing new cogging torque reduction methods.

The rest of the article is organized as follows: Section II delves into the harmonic interaction principles on the basis of cogging torque generation. Section III provides an exploration of the calculation process. Section IV presents case studies on PMMs featuring diverse topologies and pole-slot combinations. Lastly, Section V summarizes the conclusions drawn.

II. Cogging Torque Model Based on HIM

A. Energy Method for Torque Calculation

In accordance with the energy method, the torque in PMMs is determined by the variation of energy [17]. Therefore, during rotor rotation, the cogging torque under open circuit conditions can be calculated as:

$$T_c = -\frac{\partial W_\delta(\omega_m t)}{\partial t} \tag{1}$$

where T_c is the cogging torque, ω_m is the mechanical angular speed of the rotor, t is the operating time, W_δ is the magnetic energy in the airgap, which can be expressed as:

$$W_\delta(\omega_m t) = \frac{1}{2\mu_0}\int B_\delta^2(\omega_m t)dV_\delta \tag{2}$$

where μ_0 is the vacuum permeability, V_δ is the airgap volume, B_δ is the airgap flux density and generated due to the interaction between rotor MMF and airgap permeance, as expressed below:

$$B_\delta(\omega_m t) = \frac{f_r(\omega_m t)\Lambda_S}{S_\delta} \tag{3}$$

where f_r is the rotor MMF, Λ_S is the airgap permeance, S_δ is the flux area.

Therefore, precise expressions for the rotor MMF and airgap permeance are essential for cogging torque calculations.

B. Rotor MMF with Fourier Series

When the rotor is rotating at speed ω_m, the rotor MMF can be expressed in Fourier series as follows

$$f_r(\omega_m t) = \sum_{\nu_r=1,3,5,\ldots}^{2n+1} F_r(\nu_r)\cos\left(\nu_r p_N(\omega_m t - \theta_m)\right) \tag{4}$$

where ν_r is the harmonic order of the MMF, for symmetrical poles, $\nu_r = 1,3,5,\ldots,(2n+1)$. $F_r(\nu_r)$ is the amplitude of the ν_r -th order of rotor MMF, p_N is the number of pole-pairs, θ_m is the spatial angle. The order and amplitude of rotor MMF harmonics are determined by rotor parameters such as PM width and thickness, the shape of flux barrier, etc.

C. Airgap Permeance with Fourier Series

The airgap permeance is inversely proportional to the flux distance, showing a large permeance under the teeth and a small permeance under the slot opening, with a trapezoidal distribution in one slot region.

The airgap permeance considering slotting effect is given by

$$\Lambda_S = \sum_{\nu_s=0,1,2,\ldots}^{m} A_S(\nu_s)\cos(\nu_s N_S \theta_m) \tag{5}$$

where ν_s is the harmonic order of the airgap permeance, $\nu_s = 0,1,2,\ldots,m$, $A_S(\nu_s)$ is the amplitude of the ν_s -th airgap permeance. N_S is the number of slots.

The order and amplitude of airgap permeance harmonics are mainly determined by the shape of slot openings.

D. Cogging Torque Model Based on HIM

By substituting (4) and (5) into (3) and (2), the airgap energy can be derived and expressed as the following general form:

$$\begin{aligned} W_\delta(\omega_m t) &= \frac{l_\delta R_\delta l_m}{2\mu_0}\int_0^{2\pi}\left(\frac{f_r(\omega_m t)\Lambda_S}{S_\delta}\right)^2 d\theta_m \\ &= \frac{l_\delta R_\delta l_m}{16\mu_0 S_\delta^2}\sum_{i=1}^{8} W_{Ci} \end{aligned} \tag{6}$$

where l_δ , R_δ , l_m are the airgap thickness, radius of airgap center circle, and motor length, respectively. $W_C(i)_{i=1,\ldots,8}$ is the cogging torque energy component, which can be express as

$$\begin{aligned} W_{C1} &= P\int_0^{2\pi}\cos\left[Aw_m t - \left(A+C\right)\theta_m\right]d\theta_m \\ W_{C2} &= P\int_0^{2\pi}\cos\left[Aw_m t - \left(A+D\right)\theta_m\right]d\theta_m \\ W_{C3} &= P\int_0^{2\pi}\cos\left[Aw_m t - \left(A-C\right)\theta_m\right]d\theta_m \\ W_{C4} &= P\int_0^{2\pi}\cos\left[Aw_m t - \left(A-D\right)\theta_m\right]d\theta_m \\ W_{C5} &= P\int_0^{2\pi}\cos\left[Bw_m t - \left(B+C\right)\theta_m\right]d\theta_m \\ W_{C6} &= P\int_0^{2\pi}\cos\left[Bw_m t - \left(B+D\right)\theta_m\right]d\theta_m \\ W_{C7} &= P\int_0^{2\pi}\cos\left[Bw_m t - \left(B-C\right)\theta_m\right]d\theta_m \\ W_{C8} &= P\int_0^{2\pi}\cos\left[Bw_m t - \left(B-D\right)\theta_m\right]d\theta_m \end{aligned} \tag{7}$$

and

$$\begin{aligned} P &= \sum_{\nu_{r1}}\sum_{\nu_{r2}}\sum_{\nu_{s1}}\sum_{\nu_{s2}} F_r(\nu_{r1})F_r(\nu_{r2})A_S(\nu_{s1})A_S(\nu_{s2}) \\ A &= \sum_{\nu_{r1}}\sum_{\nu_{r2}}\left(\nu_{r1}+\nu_{r2}\right)p_N, \quad B = \sum_{\nu_{r1}}\sum_{\nu_{r2}}\left(\nu_{r1}-\nu_{r2}\right)p_N \\ C &= \sum_{\nu_{s1}}\sum_{\nu_{s2}}\left(\nu_{s1}+\nu_{s2}\right)N_S, \quad D = \sum_{\nu_{s1}}\sum_{\nu_{s2}}\left(\nu_{s1}-\nu_{s2}\right)N_S \end{aligned} \tag{8}$$

It's apparent that the integral in equation (7) is non-zero only when the component associated with θ_m is zero. Hence, for energy components that induce cogging torque, the following conditions must hold:

$$A = \pm C, \quad \text{or } A = \pm D, \quad \text{or } B = \pm C, \quad \text{or } B = \pm D \tag{9}$$

In this scenario, cogging torque can be generated. Referring to (1), the cogging torque can be determined as:

$$T_c = \frac{\pi l_\delta R_\delta l_m \omega_m}{8\mu_0 S_\delta^2}\sum P\left(A\sin\left(A\omega_m t\right) + B\sin\left(B\omega_m t\right)\right) \tag{10}$$

Therefore, solving for the cogging torque entails obtaining the amplitude of each harmonic of the rotor MMF and the airgap permeance.

In contrast to conventional methods, the proposed HIM-based model establishes a link between field harmonics and cogging torque. Thus, utilizing this model enables the reduction of cogging torque by adjusting either the rotor MMF or airgap permeance harmonics. Typical approaches include constructing rotor flux harmonics [1], constructing permeance harmonics, and altering the least common multiple of harmonic interactions.

III. Proposed Calculation Method for Field Harmonics and Cogging Torque

As previously discussed, accurately calculating cogging torque necessitates obtaining rotor MMF and reluctance harmonics. This section elaborates on a detailed harmonic acquisition and separation approach based on static-magnetic field FEM.

During the calculation process, the numerical model requires two static magnetic field solutions to determine the rotor MMF and airgap permeance: the airgap flux density under toothed and toothless conditions. These flux densities can be expressed as:

$$B_{\delta 1} = \frac{f_r\Lambda_S}{S_\delta}, \quad B_{\delta 0} = \frac{f_r\Lambda_{S0}}{S_\delta} \tag{11}$$

where Λ_{S0} is the airgap reluctance of toothless motor, which is a constant value.

Additionally, the harmonic content of rotor MMF can be obtained through fast-Fourier transformation (FFT) analysis on the toothless motor flux density:

$$\begin{aligned} B_{\delta 0} &= \sum_{\nu_r=1,3,\ldots}^{2n+1} B_{M\delta 0}(\nu_r) \\ &= \frac{\Lambda_{S0}}{S_\delta} \sum_{\nu_r=1,3,\ldots}^{2n+1} F_r(\nu_r)\cos\left(\nu_r p_N(\omega_m t-\theta_m)\right) \end{aligned} \tag{12}$$

where $B_{M\delta 0}$ is the amplitude of flux density harmonics.

By dividing the two flux densities, followed by further FFT analysis, the ratio of reluctance harmonics can be derived:

$$\begin{aligned} r_{\Lambda S} &= \sum_{\nu_s=0,1,2,\ldots}^{m} r_{M\Lambda S}(\nu_s) \\ &= \frac{B_{\delta 1}}{B_{\delta 0}} = \frac{\Lambda_S}{\Lambda_{S0}} = \frac{\sum_{\nu_s=0,1,2,\ldots}^{m} A_S(\nu_s)\cos(\nu_s N_S \theta_m)}{\Lambda_{S0}} \end{aligned} \tag{13}$$

Consequently, the harmonic product of the rotor MMF and airgap reluctance of any order can be determined from the harmonic components in (12) and (13), related as

$$\frac{F_r(\nu_r)\Lambda_S(\nu_s)}{S_\delta} = B_{M\delta 0}(\nu_r) r_{M\Lambda S}(\nu_s) \tag{14}$$

This leads to the derivation of the cogging torque:

$$\begin{aligned} T_c = \frac{l_\delta R_\delta l_m \pi}{8\mu_0} \sum_{\nu_{r1}}\sum_{\nu_{r2}}\sum_{\nu_{s1}}\sum_{\nu_{s2}} B_{M\delta 0}(\nu_{r1}) B_{M\delta 0}(\nu_{r2}) \times \\ r_{M\Lambda S}(\nu_{s1}) r_{M\Lambda S}(\nu_{s2}) \left(A\sin\left(A\omega_m t\right) + B\sin\left(B\omega_m t\right)\right) \end{aligned} \tag{15}$$

The proposed field harmonic and cogging torque calculation process is illustrated in Fig. 1.

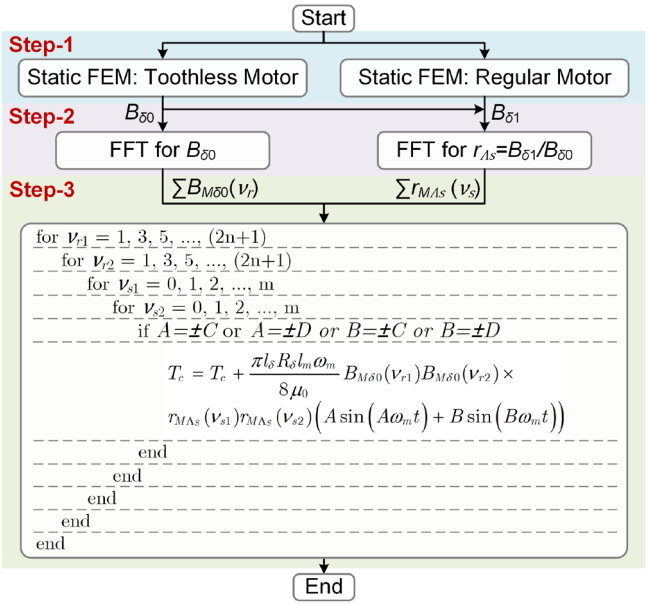

Fig. 1. Flowchart of the field harmonic and cogging torque calculation process.

IV. Cases of Verification

To validate the precision of the proposed HIM-based cogging torque model, various case studies are conducted involving different pole-slot combinations and rotor topologies.

All cases maintain identical dimensional proportions, with consistent structural parameters as detailed in Table I.

TABLE I
Uniform Structural Parameters of Case Studies

Parameter	Value	Parameter	Value
Motor outer diameter (mm)	150	Motor length (mm)	60
Airgap thickness (mm)	1	Ratio of stator bore (Inner stator to outer stator)	0.6
Ratio of tooth width (Tooth width to maximum allowable tooth width)	0.5	Ratio of slot opening (Slot opening width to allowable opening width)	0.3

A. Case I: 8-pole 24-slot V-shape IPM Machine

In this case study, an 8-pole 24-slot V-shape IPM machine is investigated. A parametric model is utilized to explore the correlation between structural parameters and cogging torque.

To verify the predictive accuracy of the proposed HIM, the V angle parameter (α_V), which denotes the angle between two PMs in a pole region, is varied from 100 degrees to 180 degrees. At 180 degrees, the PM pole transforms into a bar-type structure.

Cogging torque calculations are performed using both FEM and the proposed HIM. Comparative results displayed in Fig. 2 demonstrate consistent peak cogging torque values across different V angles. Additionally, the cogging torque waveforms for V angles of 100 and 180 degrees exhibit strong agreement.

Furthermore, the HIM showcases notable time efficiency by requiring only two static field solutions per computation. As a result, the total time for parametric exploration is reduced significantly, from 201.8 seconds to 18.8 seconds. It is noteworthy that the consumed time encompasses structural modeling, meshing, and FEM calculation. Notably, both methods share identical durations for modeling and meshing, with the discrepancy arising in the FEM calculation phase.

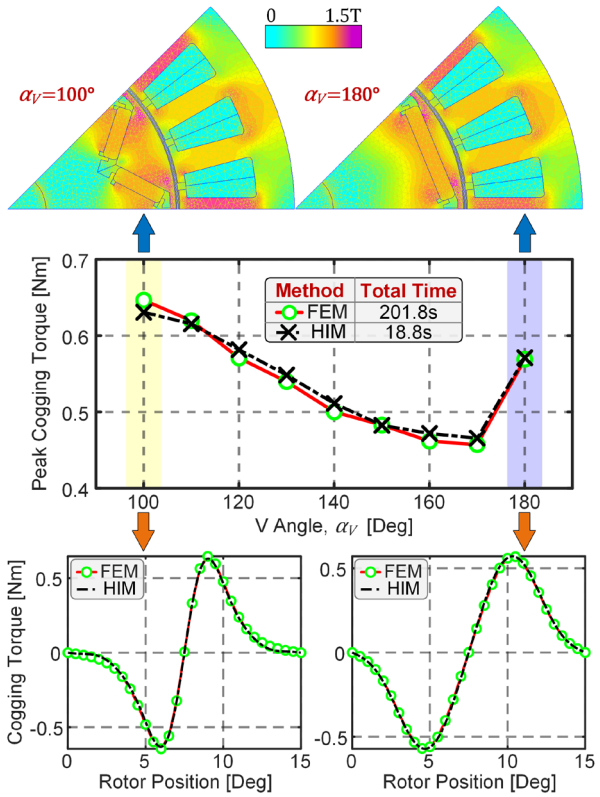

Fig. 2. Motor structures and cogging torque results for varying the PM intersecting angle ratio using FEM and HIM in Case I.

In addition to the parameter α_V, other influential factors on cogging torque include the slot opening ratio (the ratio of the slot opening width to the available slot opening width) and the PM width ratio (the ratio of PM width to the maximum PM width in a fixed cavity). These parameters are treated as variables, and their relationships with cogging torque are illustrated in Fig. 3 and Fig. 4.

Comparisons with the FEM solution reveal that the proposed method demonstrates strong consistency while substantially reducing computation time.

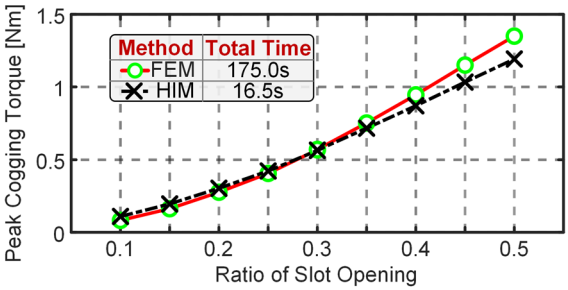

Fig. 3. Calculated peak cogging torque for varying slot opening ratios using both methods in Case I.

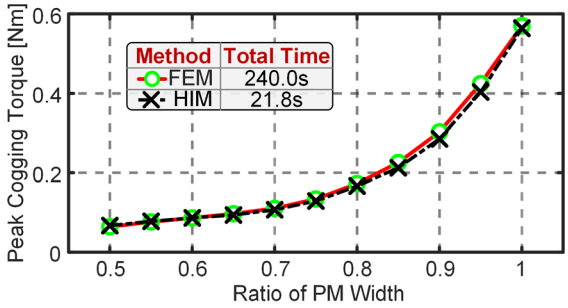

Fig. 4. Calculated peak cogging torque for different PM width ratios using both methods in Case I.

B. Case II: 8-pole 48-slot U-shape IPM Machine

In the second case, a common pole-slot configuration widely utilized in electric vehicles is examined for its benefits in minimizing cogging torque, torque ripple, and field spatial harmonics. This setup features a U-shaped PM structure, with each PM layer comprising three PMs to enhance flux density and torque density.

The initial structural parameter under investigation is the web width ratio (W_b), representing the ratio of the web width between pole-pairs to the available width. A smaller W_b indicates a larger pole-arc ratio. This ratio affects the spacing between PM poles and alters the rotor MMF harmonic characteristics. Ranging from 0.1 to 0.5, the corresponding peak cogging torques, cogging torque waveforms, and motor structures for W_b=0.1 and W_b=0.5 are shown in Fig. 5. Comparative analysis highlights the significant impact of this parameter on cogging torque, with HIM and FEM methods showing consistent and aligned results.

Furthermore, to explore the impact of airgap reluctance harmonics on cogging torque, the slot opening ratio parameter is adjusted from 0.1 to 0.5. Comparative results obtained using FEM and HIM are depicted in Fig. 6, showcasing consistent outcomes between the two methods.

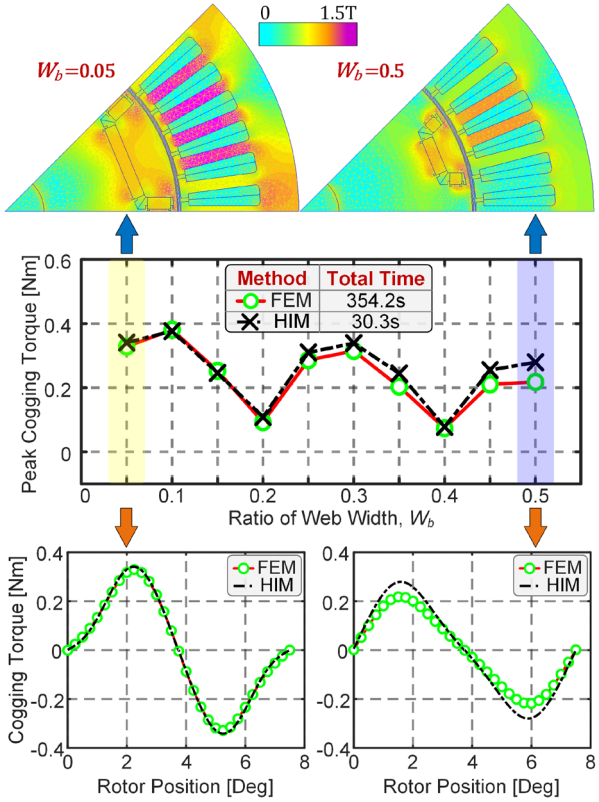

Fig. 5. Motor structures and cogging torque results for varying the ratio of PM web width using both methods in Case II.

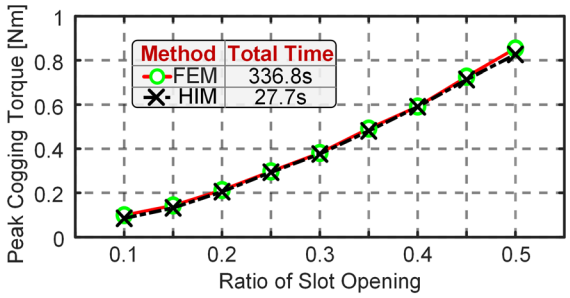

Fig. 6. Calculated peak cogging torque for varying slot opening ratios using both methods in Case II.

C. Case III: 8-pole 24-slot Double-U IPM Machine

To validate the effectiveness of the proposed method with intricate rotor structures, a double-U shaped rotor topology is investigated. This configuration features two layers of U-type PM cavities, introducing more complex rotor MMF harmonics.

The focus is on the ratio of the web width of the inner PM layer, ranging from 0.35 to 0.55. Results obtained from FEM and HIM are depicted in Fig. 7, showcasing peak cogging torque, cogging torque waveforms, and motor structures. Comparative analysis reveals good agreement across different values of the inner PM web width ratio, affirming the effectiveness of the proposed method in analyzing complex rotor structures.

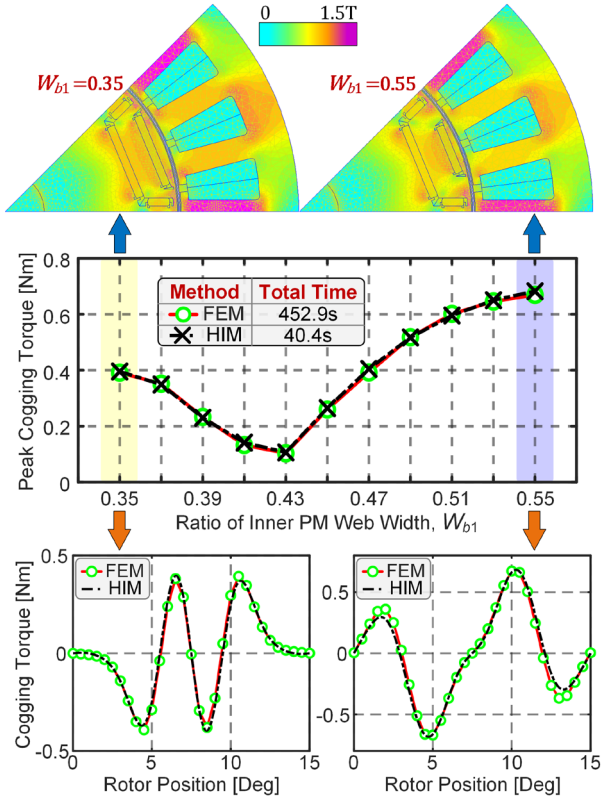

Fig. 7. Motor structures and cogging torque results for varying the ratio of inner layer web width between the two methods in Case III.

In summary, the three case studies demonstrate that the proposed HIM accurately predicts cogging torque while requiring less computational time.

V. Conclusion

This paper proposes a semi-analytical method for the cogging torque calculation based on the harmonic interaction effect, which solves for the cogging torque by analyzing the Fourier expansions of the rotor MMF with motion and the airgap permeance with the slotting effect.

The key findings are as follows:

1. The HIM-based approach offers accurate predictions and rapid calculations, saving over 90% of computation time compared to traditional FEM methods. This is particularly advantageous for rapid analysis of axial-flux PMMs, where 3D FEM can be time-consuming, and is also beneficial for large-scale optimization.
2. The proposed method is user-friendly and demonstrates broad applicability across diverse rotor structures. This distinguishes it from existing analytical models.
3. By establishing a straightforward link between rotor MMF harmonics, airgap permeance harmonics, and cogging torque frequencies, this method establishes a solid theoretical foundation for the development of cogging torque suppression techniques.
4. Further exploration is warranted into predicting on-load torque ripple through the analysis of harmonic interaction laws. This will contribute to the enrichment of the HIM-based torque analysis mechanism.

Acknowledgement

This work was supported by National Natural Science Foundation of China under Project 52077187.

References

[1] L. Dai, J. Gao, S. Niu, K. Liu, S. Huang and W. L. Chan, "Cogging Torque Suppression for IPMSM Based on Flux Harmonic Configuration," *IEEE Trans. Ind. Electron.*, Early Access, doi: 10.1109/TIE.2024.3443959.

[2] S. A. Saied, K. Abbaszadeh, A. Tenconi and S. Vaschetto, "New Approach to Cogging Torque Simulation Using Numerical Functions," *IEEE Trans. Ind. Appl.*, vol. 50, no. 4, pp. 2420-2426, July-Aug. 2014.

[3] F. Ebadi, M. Mardaneh, A. Rahideh and N. Bianchi, "Analytical Energy-Based Approaches for Cogging Torque Calculation in Surface-Mounted PM Motors," *IEEE Trans. Magn.*, vol. 55, no. 5, pp. 1-10, May 2019, Art no. 8101410.

[4] Z. Q. Zhu, L. J. Wu and Z. P. Xia, "An Accurate Subdomain Model for Magnetic Field Computation in Slotted Surface-Mounted Permanent-Magnet Machines," *IEEE Trans. Magn.*, vol. 46, no. 4, pp. 1100-1115, April 2010.

[5] L. J. Wu, Z. Q. Zhu, D. A. Staton, M. Popescu and D. Hawkins, "Comparison of Analytical Models of Cogging Torque in Surface-Mounted PM Machines," *IEEE Trans. Ind. Electron.*, vol. 59, no. 6, pp. 2414-2425, June 2012.

[6] Y. Zhou, H. Li, G. Meng, S. Zhou and Q. Cao, "Analytical Calculation of Magnetic Field and Cogging Torque in Surface-Mounted Permanent-Magnet Machines Accounting for Any Eccentric Rotor Shape," *IEEE Trans. Ind. Electron.*, vol. 62, no. 6, pp. 3438-3447, June 2015.

[7] H. Qian, H. Guo, Z. Wu and X. Ding, "Analytical Solution for Cogging Torque in Surface-Mounted Permanent-Magnet Motors With Magnet Imperfections and Rotor Eccentricity," *IEEE Trans. Magn.*, vol. 50, no. 8, pp. 1-15, Aug. 2014, Art no. 8201615.

[8] A. J. Piña Ortega, S. Paul, R. Islam and L. Xu, "Analytical Model for Predicting Effects of Manufacturing Variations on Cogging Torque in Surface-Mounted Permanent Magnet Motors," *IEEE Trans. Ind. Appl.*, vol. 52, no. 4, pp. 3050-3061, July-Aug. 2016.

[9] S. Li, W. Tong, S. Wu and R. Tang, "Analytical Model for Electromagnetic Performance Prediction of IPM Motors Considering Different Rotor Topologies," *IEEE Trans. Ind. Appl.*, vol. 59, no. 4, pp. 4045-4055, July-Aug. 2023.

[10] Y. Du, Y. Huang, B. Guo, F. Peng, Y. Yao and J. Dong, "Magnetic Field Prediction of U-Shaped Interior Permanent Magnet Motor Considering Magnetic Bridge Saturation," *IEEE Trans. Magn.*, vol. 60, no. 3, pp. 1-4, March 2024, Art no. 8200304.

[11] M. Hajdinjak and D. Miljavec, "Analytical Calculation of the Magnetic Field Distribution in Slotless Brushless Machines With U-Shaped Interior Permanent Magnets," *IEEE Trans. Ind. Electron.*, vol. 67, no. 8, pp. 6721-6731, Aug. 2020.

[12] P. Wu and Y. Sun, "A Novel Analytical Model for On-Load Performance Prediction of Delta-Type IPM Motors Based on Rotor Simplification," in *IEEE Trans. Ind. Electron.*, vol. 71, no. 7, pp. 6841-6851, July 2024.

[13] J. H. Seo and H. S. Choi, "Cogging Torque Calculation for IPM Having Single Layer Based on Magnetic Circuit Model," *IEEE Trans. Magn.*, vol. 50, no. 10, pp. 1-4, Oct. 2014, Art no. 8102104.

[14] C. Ma et al., "Analytical Model of Open-Circuit Air-Gap Field Distribution in Interior Permanent Magnet Machines Based on Magnetic Equivalent Circuit Method and Boundary Conditions of Macroscopic Equations," *IEEE Trans. Magn.*, vol. 57, no. 3, pp. 1-9, March 2021, Art no. 8104209.

[15] S. Li, W. Tong, M. Hou, S. Wu and R. Tang, "Analytical Model for No-Load Electromagnetic Performance Prediction of V-Shape IPM Motors Considering Nonlinearity of Magnetic Bridges," *IEEE Trans. Energy Convers.*, vol. 37, no. 2, pp. 901-911, June 2022.

[16] Z. Xiang, Y. Zhou, X. Zhu, L. Quan, D. Fan and Q. Liu, "Research on Characteristic Airgap Harmonics of a Double-Rotor Flux-Modulated PM Motor Based on Harmonic Dimensionality Reduction," *IEEE Trans Transport. Electrific.*, vol. 10, no. 3, pp. 5750-5761, Sept. 20248.

[17] L. Dai, S. Niu, W. Zhang, J. Gao and S. Huang, "Harmonic Modeling and Ripple Suppression of Electromagnetic Torque in IPMSMs," *IEEE Trans. Ind. Electron.*, vol. 71, no. 12, pp. 16223-16233, Dec. 2024.